STELLAR MODELS II: HOMOLOGY

10.1   Introduction

As we have seen in the previous lecture, there are no straightforward analytic solutions to the equations of stellar structure. Rather, the equations are solved iteratively with numerical methods, a process that can be quite consuming in terms of computing resources. However, one important property of the equations is that they are *homologous.* Homology means that, given a solution to the equations—whereby the quantities $(P, T, L,$ and $\rho)$ are specified as a function of the radial coordinate r (in the Eulerian formulation) or as a function of m (Lagrangian formulation) for a star of total mass M and of a given chemical composition (this is what constitutes a stellar model), then we can find a new solution for a star of a different total mass M' simply by multiplying the other physical variables by appropriate scaling factors.

This approach is adequate if, for example, we are interested in reproducing the stellar mass-luminosity relationship (Figure 4.8), or the Main Sequence of hydrogen burning stars in the luminosity-temperature diagram (Figure 3.6). Of course, the implicit assumption in homologous stellar models is that stars have the same chemical composition, but this is approximately the case for most stars on the Main Sequence in the solar neighbourhood.

Physically, in two stars related by a homology transformation we assume that the *way* in which a physical quantity varies from the centre of a star to its surface is the same for all stars, irrespectively of the total stellar mass. For example, the increase of luminosity with radius reduces to a single curve (Figure 10.1) when plotted as a function of the *fractional* mass $x = m(r)/M$. In this way, any stellar model is related to an initial (or reference) one by a simple change in scale.
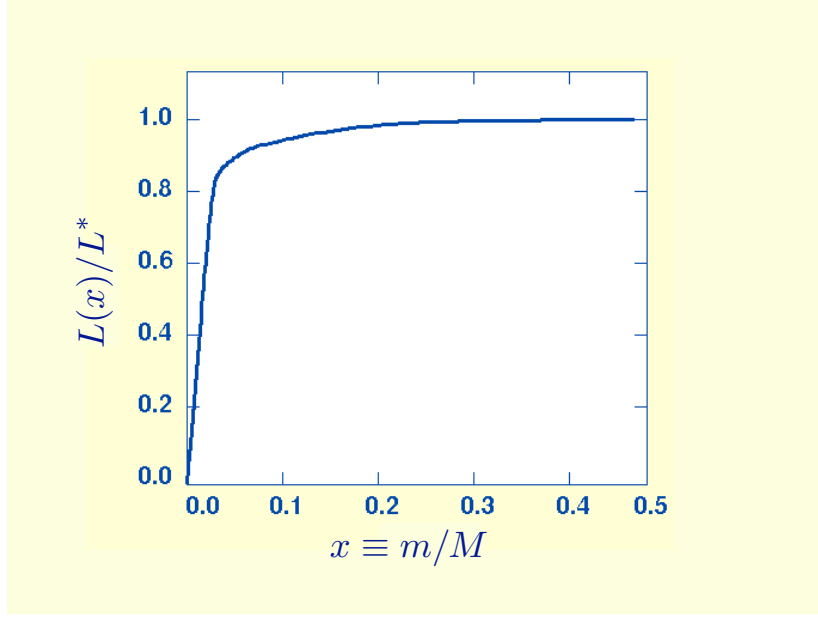
Figure 10.1: In homologous stellar models the growth of fractional luminosity with fractional stellar mass is the same for all stars, irrespectively of a star's total luminosity L and total mass M.

10.2   An example

Consider two stars with masses M_1 and M_2 and radii R_1 and R_2. We define:

$$x' = \frac{r_1}{R_1} = \frac{r_2}{R_2}\,. \tag{10.1}$$

Then,

$$x \equiv \frac{m_1(r_1)}{M_1} = \frac{m_2(r_2)}{M_2} \tag{10.2}$$

expresses the fact that each star contains the same fraction x of its mass within the same fraction x' of its radius.

Let us now consider the homology transformation of the first equation of stellar structure, the equation of mass continuity. In Euler coordinates, we have for star 1:

$$\frac{dm_1}{dr_1} = 4\pi r_1^2\,\rho_1 \tag{10.3}$$

which may be transformed for star 2 as:

$$\frac{dm_2}{dr_2} = \frac{M_2}{M_1}\frac{dm_1}{dr_2} = \frac{M_2}{M_1}\frac{R_1}{R_2}\frac{dm_1}{dr_1}\,. \tag{10.4}$$

But we also have:

$$\frac{dm_2}{dr_2} = 4\pi r_2^2\,\rho_2 = 4\pi\left(\frac{R_2}{R_1}\right)^2 r_1^2\,\rho_2\,. \tag{10.5}$$

2

Equating the r.h.s. of the last two equations, we have:

$$\frac{dm_1}{dr_1} = 4\pi r_1^2 \frac{M_1}{M_2} \left(\frac{R_2}{R_1}\right)^3 \rho_2 \tag{10.6}$$

Comparing 10.3 and 10.6, it can be seen immediately that the density of star 2 at x can be obtained by scaling the density at x of star 1:

$$\rho_2(x) = \left(\frac{M_2}{M_1}\right) \left(\frac{R_1}{R_2}\right)^3 \rho_1(x). \tag{10.7}$$

10.3 Homologous Transformations

More generally (and working now in Lagrangian coordinates), we can replace the solutions to the four equations of stellar structure plus the constitutive equation for density, $r(m)$, $P(m)$, $L(m)$, $T(m)$ and $\rho(m)$, with five relations as follows:

$$\begin{aligned}
r &= f_1(x) \cdot R^* \\
P &= f_2(x) \cdot P^* \\
L &= f_3(x) \cdot L^* \\
T &= f_4(x) \cdot T^* \\
\rho &= f_5(x) \cdot \rho^*
\end{aligned} \tag{10.8}$$

where R^*, P^*, L^*, T^*, ρ^* are dimensional coefficients for, respectively, the radius, pressure, luminosity, temperature and density, and the $f_n(x)$ are the (dimensionless) scaling functions. By definition, $f_n(x) = 0\text{--}1$; with f_1 and $f_3 = 1$ when $x = 1$, and f_2, f_4, and $f_5 = 1$ when $x = 0$.

Consider the equation of hydrostatic equilibrium:

$$\frac{dP}{dm} = -\frac{Gm}{4\pi r^4} \tag{10.9}$$

With the substitutions: $dP = df_2 \cdot P^*$, $dm = dx \cdot M$, $m = x \cdot M$, and $r = f_1 \cdot R^*$, it becomes:

$$\frac{df_2}{dx} \cdot \frac{P^*}{M} = -\frac{GM x}{4\pi f_1^4 (R^*)^4}$$

or

$$\frac{df_2}{dx} = -\frac{x}{4\pi f_1^4} \cdot \frac{GM^2}{(R^*)^4 P^*}. \tag{10.10}$$

3

The advantage of this formulation is that it clearly separates the stellar structure aspect (the first term on the r.h.s. of the equation) from the scaling between stars of different masses (the second term on the r.h.s.). Recalling that the f_n functions are dimensionless, all the dimensions are in the second term on the r.h.s., which therefore implies:

$$P^* = \frac{GM^2}{(R^*)^4}$$

Repeating this procedure for the four equations of stellar structure (ignoring convection and radiation pressure), we have five pairs of equations, as follows:

$$\frac{df_1}{dx} = \frac{1}{4\pi f_1^2 f_5}; \qquad \rho^* = \frac{M}{(R^*)^3} \tag{10.11}$$

$$\frac{df_2}{dx} = -\frac{x}{4\pi f_1^4}; \qquad P^* = \frac{GM^2}{(R^*)^4} \tag{10.12}$$

$$\frac{df_3}{dx} = f_5 f_4^{\beta}; \qquad L^* = \mathcal{E}_0\, \rho^*(T^*)^{\beta} M \tag{10.13}$$

$$\frac{df_4}{dx} = -\frac{3f_3}{4f_4^3 \left(4\pi f_1^2\right)^2}; \qquad L^* = \frac{ac}{\kappa} \frac{(T^*)^4 (R^*)^4}{M} \tag{10.14}$$

$$f_5 = \frac{f_2}{f_4}; \qquad T^* = \frac{\mu m_H}{k} \frac{P^*}{\rho^*} \tag{10.15}$$

Note that the equations on the l.h.s. constitute a set of nonlinear differential equations which are independent of M. On the r.h.s. we have five algebraic equations which relate the dimensional coefficients R^*, P^*, ...; these coefficients can be manipulated to obtain the dependence on M of the property of interest. Some pertinent examples follow.

10.3.1   Mass-Luminosity Relation

Substituting the expressions for ρ^* and P^* from 10.11 and 10.12 into 10.15, we obtain:

$$T^* = \frac{\mu m_H}{k} \frac{GM^2}{(R^*)^4} \frac{(R^*)^3}{M} = \frac{\mu m_H}{k} \frac{GM}{R^*} \tag{10.16}$$

Using this expression for T^* in eq. 10.14, we have:

$$L^* = \frac{ac}{\kappa} \left(\frac{\mu m_H G}{k}\right)^4 \cdot \frac{M^4 (R^*)^4}{M (R^*)^4} \tag{10.17}$$

The above equation is valid at any value of x (the fractional mass). But since $f_3(x) = 1$, when $x = 1$, we obtain the mass-luminosity relationship:

$$L \propto M^3 \tag{10.18}$$

Equation 10.18 is not a bad approximation to the real $M - L$ relationship we found in Lecture 4 and shown again here in Figure 10.2, considering that we have ignored convection and radiation pressure.[1]
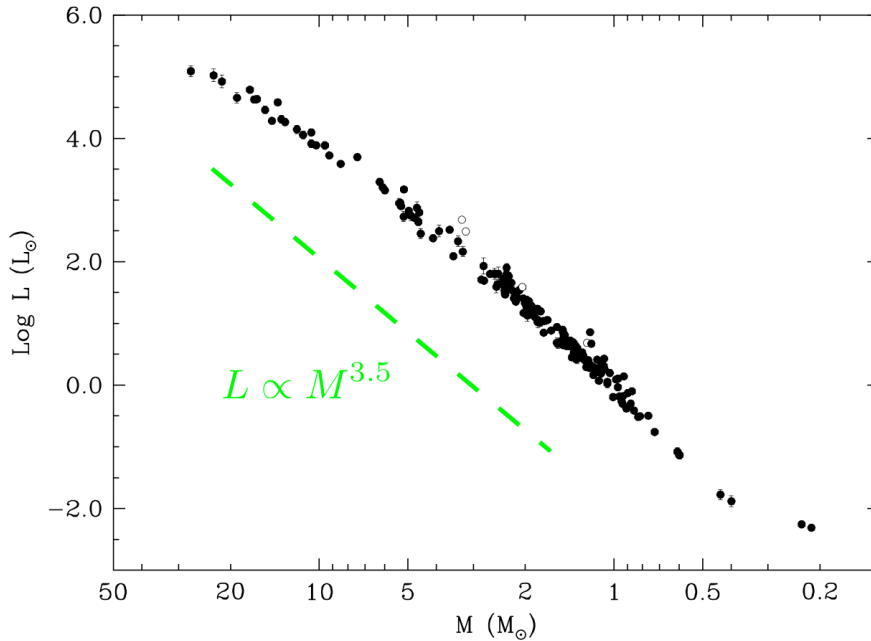

Figure 10.2: The empirical stellar mass-luminosity relation constructed from observations of 190 binary stars with well-determined parameters. (Reproduced from Torres et al. 2010).

Note that there is a real spread to the M-L relation, better seen in Figure 10.3: at each value of mass there a spread in luminosity which is much larger than the observational error. The spread is thought to be due to stellar evolution *during the main sequence lifetime*, as well as to the fact that not all the stars in the plot have the same chemical composition.

---

[1]Note also that in going from 10.17 to 10.18 we have treated the opacity κ as a constant. For simplicity, we shall assume $\kappa \approx$ const throughout section 10.3 even though, as we saw in Lecture 5, the mean opacity follows a Kramers' law: $\langle \kappa \rangle \propto \rho T^{-3.5}$ (see Figure 5.5). A more rigourous treatment would include the density and temperature dependence of the opacity in the scaling relations.
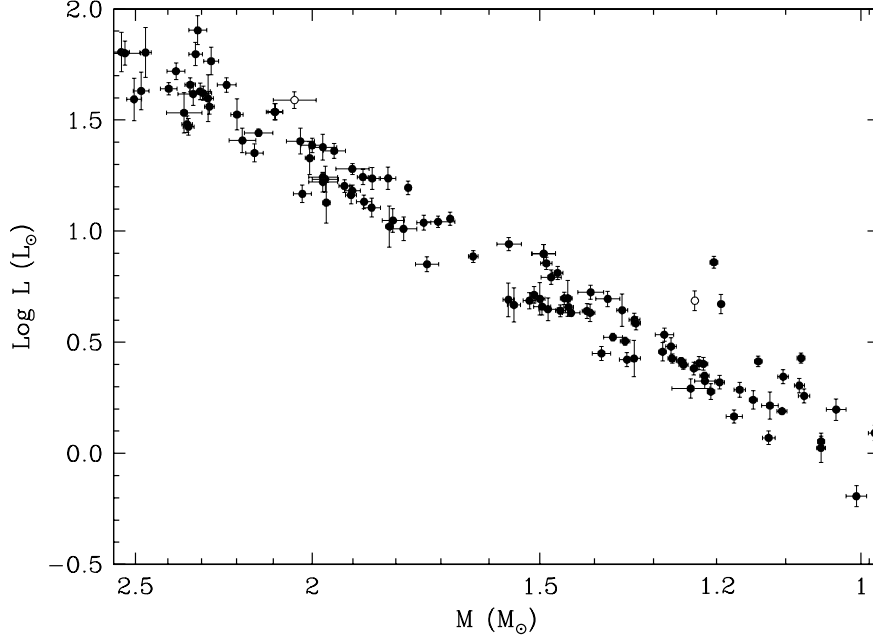
Figure 10.3: Close-up of the 1–2.5$M_\odot$ range of the mass-luminosity relation of Torres et al. 2010. The very significant (in the sense that it is many times the typical error) scatter in $\log L$ at each mass value is due to the combined effects of stellar evolution and abundance differences. Stars classified as giants are shown with open circles. (Reproduced from Torres et al. 2010).

10.3.2 Mass-Radius Relation

We have written down two equations for the luminosity:

$$L^* = \frac{ac}{\kappa} \left(\frac{\mu m_H G}{k} \right)^4 M^3 ; \qquad L^* = \mathcal{E}_0 \, \rho^* (T^*)^\beta M ; \qquad (10.19)$$

therefore:

$$\rho^* = \frac{M^2}{(T^*)^\beta} \cdot \frac{ac}{\kappa \mathcal{E}_0} \cdot \left(\frac{\mu m_H G}{k} \right)^4 , \text{ or } \qquad \rho^* \propto \frac{M^2}{(T^*)^\beta} \qquad (10.20)$$

We also have:

$$T^* \propto \frac{P^*}{\rho^*} , \quad T^* \propto \frac{M^2}{(R^*)^4} \cdot \frac{(R^*)^3}{M} , \quad T^* \propto \frac{M}{R^*} \qquad (10.21)$$

using 10.11 and 10.12. Also, from 10.11, we have:

$$(R^*)^3 \propto \frac{M}{\rho^*} , \quad (R^*)^3 \propto M \cdot \frac{(T^*)^\beta}{M^2} , \quad (R^*)^3 \propto \frac{(T^*)^\beta}{M} \qquad (10.22)$$

Thus,

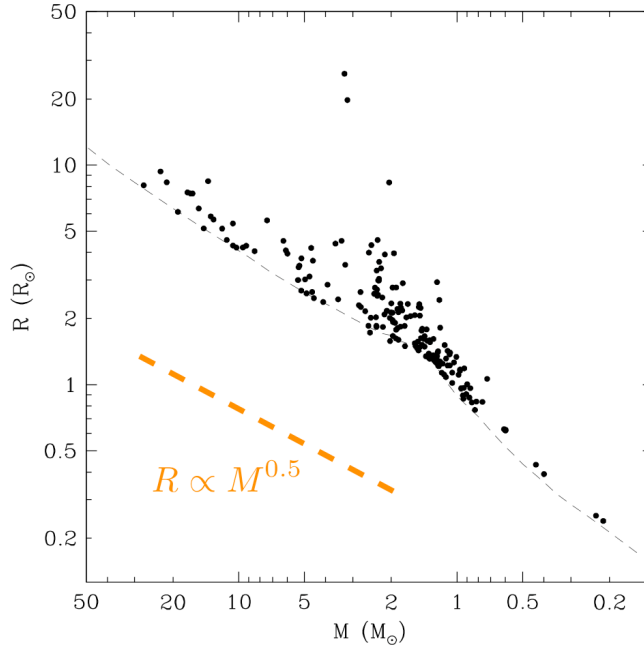$$(R^*)^3 \propto \frac{M^\beta}{M} \cdot \frac{1}{(R^*)^\beta} \qquad (10.23)$$

6

Figure 10.4: Mass-radius relation for 190 stars whose masses and radii are known to better than 3%. The faint dashed line shows a theoretical M–R relation for a zero-age Main Sequence (ZAMS) of solar metallicity, computed from a full set of stellar models. (Reproduced from Torres et al. 2010).

which gives us the mass-radius relation:

$$\boxed{R \propto M^{(\beta-1/\beta+3)}} \tag{10.24}$$

Equation 10.24 tells us that the scaling of stellar radius with mass depends on the exponent β of the power-law dependence on temperature of the rate of energy generation per unit mass of nuclear fuel (eq. 7.25). We saw in Lecture 7.4.1 that for stars burning hydrogen into helium via the p-p chain, $\beta = 4$. Thus for these stars:

$$R \propto M^{3/7}$$

High mass stars burn H into He via the CNO cycle with $\beta = 17$, leading to:

$$R \propto M^{16/20}$$

These scaling are not too dissimilar from the empirical mass-radius relation derived for the same set of well observed stars in binary systems already considered in section 10.3.1, from the compilation by Torres et al. 2010 (A&ARv, 18, 67), as can be seen from Figure 10.4.

Since the density is just mass over volume, we have the scaling of density with mass:

$$\rho^* = \frac{M}{(R^*)^3}, \quad \rho^* \propto M^{(6-2\beta/\beta+3)}$$

from which we see that more massive stars have lower densities for $\beta > 3$, i.e. even for hydrogen burning via the p-p chain.

10.3.3 Luminosity-Temperature Relation

With the mass-luminosity and mass-radius relations just derived we can now make an approximate prediction for the slope of the Main Sequence in the Luminosity-Temperature relation (i.e. the H-R diagram). Recalling that:

$$L = 4\pi R^2 \sigma T_{\text{eff}}^4 \tag{10.25}$$

we obtain, combining 10.25, 10.18 and 10.24:

$$L^{1-\frac{2(\beta-1)}{3(\beta+3)}} \propto T_{\text{eff}}^4 \tag{10.26}$$

which implies

$$\log L = 5.6 \log T_{\text{eff}} + \mathcal{C} \tag{10.27}$$

for stars burning H into He via the p-p chain, and

$$\log L = 8.6 \log T_{\text{eff}} + \mathcal{C}' \tag{10.28}$$

for more massive stars burning H via the CNO cycle.

Again, these are in reasonable agreement with the approximate double power-law slope of the Main Sequence for stars with masses $M \gtrsim 1 M_\odot$ (see Figure 10.5).

10.4 Minimum Stellar Mass

We can use the homologous transformations developed in Section 10.3 to estimate the mass limits of the Main Sequence. The low mass limit is determined by the minimum temperature required to ignite hydrogen fusion via the p-p chain, while the upper mass limit is set by radiation pressure.
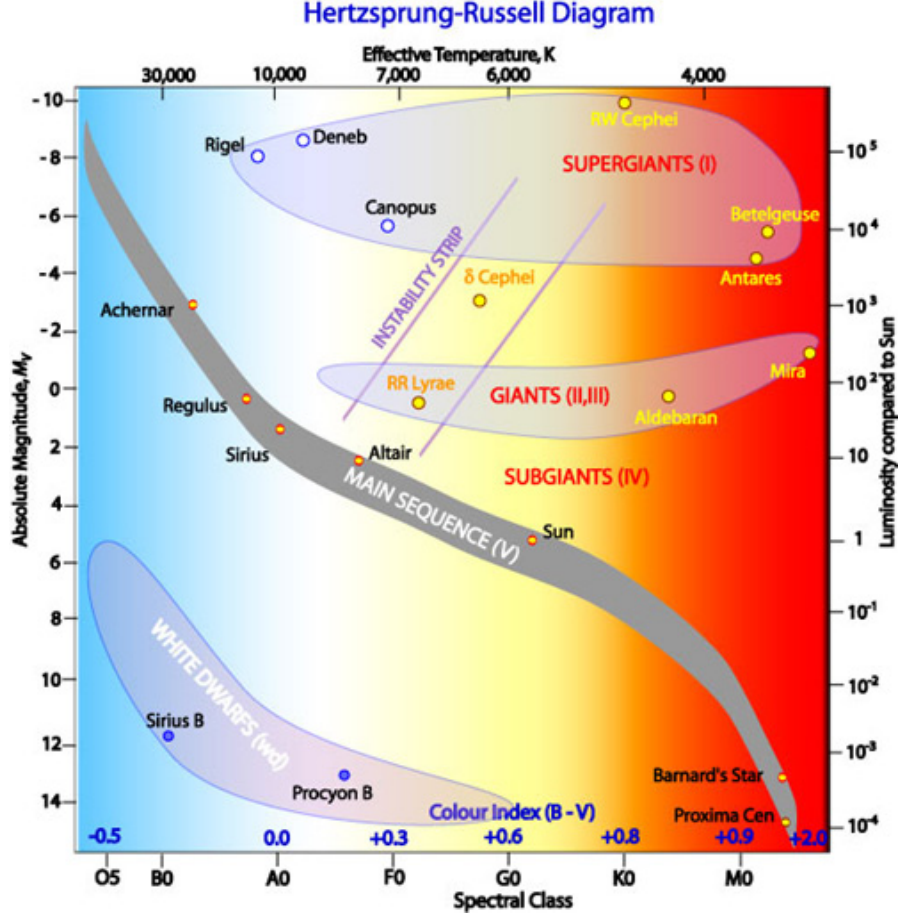
Figure 10.5: Schematic representation of the H-R diagram.

The approximate minimum temperature required for nuclear reactions to take place is $T \simeq 4 \times 10^6$ K; at lower temperatures, the protons kinetic energy is too low to bring sufficient numbers of them close enough for quantum mechanical tunneling of the Coulomb barrier to take place (Section 7.2.1).

Details models of the Sun indicate that its central temperature, $T_c \equiv T(x = 0) = 1.5 \times 10^7$ K. Using eq. 10.16 together with our mass-radius relation (10.24), we have:

$$T^* = \frac{\mu m_H}{k} \frac{GM}{R^*}; \qquad T^* \propto \frac{GM}{M^{(\beta-1/\beta+3)}}; \qquad T^* \propto M^{1-\frac{\beta-1}{\beta+3}}$$

or

$$T^* \propto M^{4/7}$$

for the p-p chain ($\beta = 4$). Thus,

$$M_{\min} = M_\odot \cdot \left(\frac{4}{15}\right)^{7/4} \simeq 0.1 \, M_\odot \tag{10.29}$$

9

Such a star will have a luminosity of only $L_{\min} \simeq 10^{-3} L_\odot$, given the $L \propto M^3$ scaling (Section 10.3.1). Furthermore, using the mass-radius relation $R \propto M^{3/7}$ appropriate to the p-p chain (eq. 10.24), together with eq. 10.25, we have:

$$L = 4\pi R^2 \, \sigma T_{\text{eff}}^4 \;\; \Rightarrow \;\; M^3 \propto M^{6/7} \, T_{\text{eff}}^4 \tag{10.30}$$

Hence:

$$T_{\text{eff}} \propto M^{15/28} \tag{10.31}$$

and

$$T_{\text{eff,min}} = T_{\text{eff},\odot} \cdot \left(\frac{M_{\min}}{M_\odot} \right)^{15/28} \simeq 5770 \times 0.1^{15/28} \simeq 1700\,\text{K} \tag{10.32}$$

In summary, scaling from the solar parameters, the low mass end of the Main Sequence of hydrogen burning stars is expected to occur at $L \sim 10^{-3} L_\odot$, $T_{\text{eff}} \sim 1700\,\text{K}$. The value of $L_{\min}$ thus derived matches observations, while that of $T_{\text{eff,min}}$ is about a factor of two too low (see Figure 10.5). One reason for the discrepancy may be the fact that, as we saw in Lecture 8.3.1, such low mass stars are almost entirely convective, and we have not included convection in our homologous transformations.

An example of a star near the low mass limit of the hydrogen burning Main Sequence is the red dwarf star Wolf 359, in the constellation of Leo (see Figure 10.6). At a distance of only 2.4 pc, Wolf 359 is the fifth closest star to the Sun, after the three stars that make up the α Centauri system and Barnard's star. Its spectral type is M6.0 V and its luminosity is $0.001 L_\odot$;
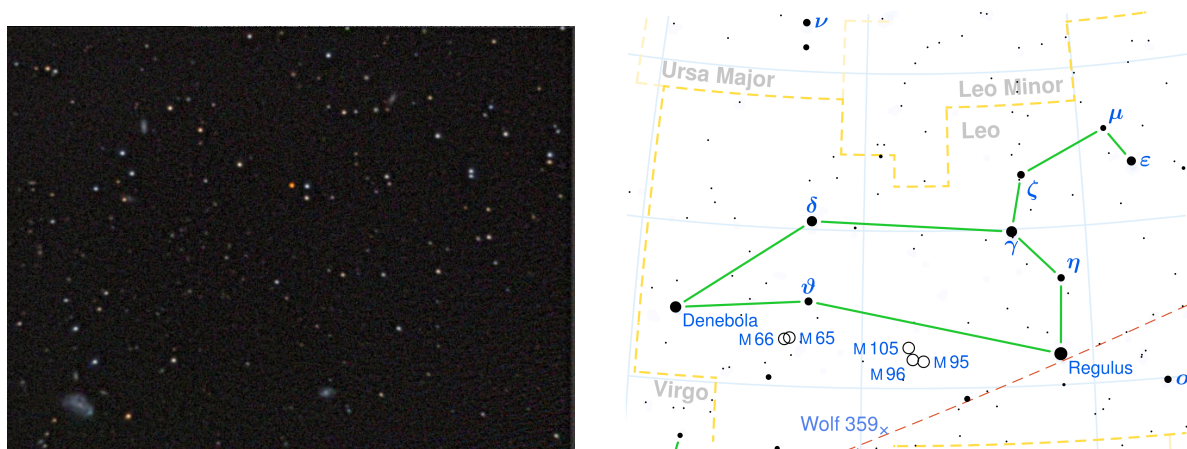

Figure 10.6: The red dwarf star Wolf 359 in the constellation of Leo is the orange-red object just above centre in the left-hand image.

if it were placed at the Sun's distance, it would be only about ten times brighter than the full Moon. The mass of Wolf 359 is $M = 0.09 M_\odot$, just above the limit of $0.08 M_\odot$ (derived more carefully than the homologous transformation above) for hydrogen fusion via the p-p chain. Its effective temperature is $T_{\text{eff}} = 2800 \pm 100$ K. Despite its proximity, Wolf 359 is a faint object at visible wavelengths, although it is brighter in the near-infrared: $V = 13.5$, but $J = 7.1$.

10.5   Eddington Luminosity

We saw in Section 9.2.2 that photons can exert pressure on the gas, so that the total pressure is the sum of two components:

$$P = P_g + P_{\text{rad}} = \frac{\rho k T}{\mu m_H} + \frac{1}{3} a T^4 \tag{10.33}$$

This equation shows that if the temperature is sufficiently high and the density is sufficiently low, radiation pressure can dominate over the gas pressure—such a situation can occur in the outer layers of very massive stars. We also saw in Lecture 8.4.1 that it is the pressure gradient within a star that counteracts the force of gravity and stops a star from collapsing onto itself.

The Cambridge astrophysicist Arthur Eddington, Plumian professor and director of the Cambridge Observatory from 1914, understood that there is a limit to the luminosity that a star can attain, beyond which the radiation pressure would exert an outward force *greater* than the inward force of gravity, rendering the star highly unstable. This upper limit to a star's luminosity is called the Eddington limit.

For a star to maintain hydrostatic equilibrium, we require:

$$\left| \frac{dP_{\text{rad}}}{dr} \right| < G \frac{M_r \rho}{r^2} \tag{10.34}$$

If radiation pressure dominates:

$$P_{\text{rad}} = \frac{1}{3} a T^4$$

$$\frac{dP_{\text{rad}}}{dT} = \frac{4}{3} a T^3 \tag{10.35}$$

Recalling the Eddington equation for radiative equilibrium:

$$\frac{dT}{dr} = -\frac{3}{4} \cdot \frac{1}{ac} \cdot \frac{\kappa\rho}{T^3} \cdot \frac{L_r}{4\pi r^2} \tag{10.36}$$

we have:

$$\frac{dP_{\text{rad}}}{dr} = -\frac{\kappa\rho}{c}\frac{L}{4\pi r^2} \tag{10.37}$$

But we also have, from the equation of hydrostatic equilibrium:

$$\frac{dP}{dr} = -G\frac{M_r\rho}{r^2} \tag{10.38}$$

Equating 10.37 and 10.38, we find:

$$\boxed{L_{\text{edd}} = 4\pi c\,G\,\frac{M}{\kappa}} \tag{10.39}$$

A star of this luminosity is supported by radiation pressure alone! And if this luminosity is exceeded, material can be peeled off the surface of the star by the transfer of momentum from photons.

The influence of radiation pressure is often expressed in terms of the *Eddington factor*:

$$\Gamma_{\text{edd}} \equiv \frac{L}{L_{\text{edd}}} = \frac{\kappa L}{4\pi c\,GM} \tag{10.40}$$

10.6 Maximum Stellar Mass

If the gas is fully ionised, the main source of opacity is electron scattering (Lecture 5.4). In Lecture 5.5, the point was made that electron scattering has no wavelength, density, nor temperature dependence, so that κ_{es} takes a particularly simple form: $\kappa_{es} = 0.2\,(1 + X)\,\text{cm}^2\,\text{g}^{-1}$, where X is the mass fraction of hydrogen. Entering the values of the physical constants in eq. 10.39, we now have:

$$\begin{aligned}
\frac{L_{\text{edd}}}{L_\odot} &= \frac{1.3 \times 10^4}{\kappa_{es}}\frac{M}{M_\odot} \\
&= \frac{1.3 \times 10^4}{0.20\,(1 + 0.7)}\frac{M}{M_\odot} \\
&\simeq 3.8 \times 10^4\,\frac{M}{M_\odot}
\end{aligned} \tag{10.41}$$

We can now use our homology transformation $L \propto M^3$, to find the maximum stellar mass:

$$M_{\max} = \sqrt{3.8 \times 10^4} \, M_\odot \; \simeq 200 M_\odot \qquad (10.42)$$

Such a star will have a luminosity:

$$L_{\max} = 7.4 \times 10^6 \, L_\odot \qquad (10.43)$$

Empirically, however, it appears that $M \simeq 100\text{--}120 M_\odot$ is a more realistic upper limit to the stellar mass (see Figure 10.7). The observed luminosity limit appears to *decrease* with decreasing effective temperature for stars with $T_{\text{eff}} \gtrsim 10\,000\,\text{K}$ and then remain approximately constant at $\log L/L_\odot \simeq 5.7$. Lamers and Fitzpatrick (1988) understood this behaviour in terms of the "Photospheric Eddington Limit". The limits deduced above apply to the case when electron scattering is the only source of opacity. But in the atmospheres of even the hottest stars, not all elements are fully ionised. Including the full effects of metal line opacities (bound-bound transitions), shows that $\langle \kappa \rangle$ *increases* from $T_{\text{eff}} = 50\,000\,\text{K}$ to $10\,000\,\text{K}$, and then drops steeply to lower T_{eff}. Once this behaviour of the full opacity is taken into account, there is excellent agreement between the Humphreys-Davidson empirical limit and the modified (or atmospheric) Eddington limit (see Figure 10.8).
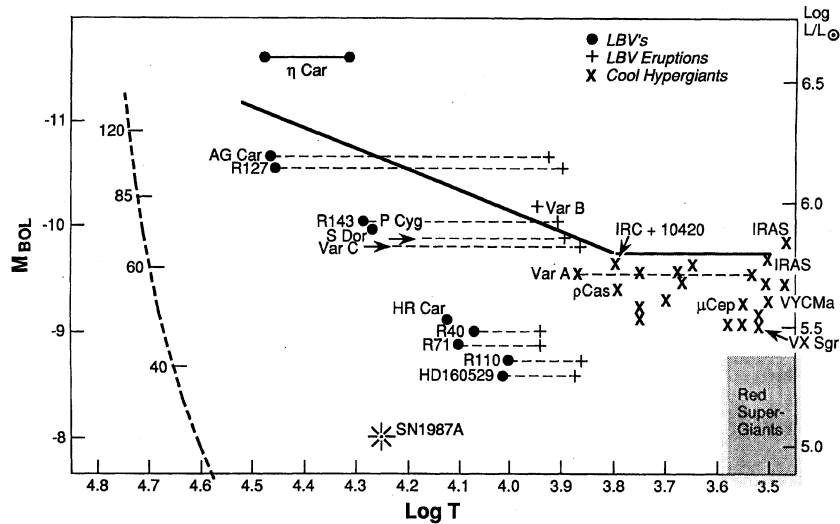

Figure 10.7: A schematic HR diagram for the most luminous known stars. The continuous black line shows the empirical upper luminosity boundary known as the Humphreys-Davidson limit. (Figure reproduced from Humphreys & Davidson 1994, PASP, 106, 1025).

13

As one might expect, the boundary set by the photospheric Eddington limit changes with metallicity.

10.6.1   Luminous Blue Variables

Luminous Blue Variable, or LBV, is a term coined by Peter Conti in 1984, to describe a class of very rare (only about 20 are known), extremely luminous blue stars which undergo outbursts, increasing their visual brightness by 1–2 magnitudes and experiencing significant mass loss, at a rate that can be as high as 10^{-2}–$10^{-1} M_\odot \, \mathrm{yr}^{-1}$. Such outbursts occur on timescales of a few decades or, in some cases, centuries, making our census of such stars very incomplete. This, coupled with their presumably very short lifetimes, explains the paucity of objects in this rare class.

During their quiescent periods, LBVs are found just on the hotter side (to the left in Figure 10.8) of the Humphreys-Davidson limit, unstable because they are near their (atmospheric) Eddington limits. However, as these stars cool and approach the Eddington limit they are not totally
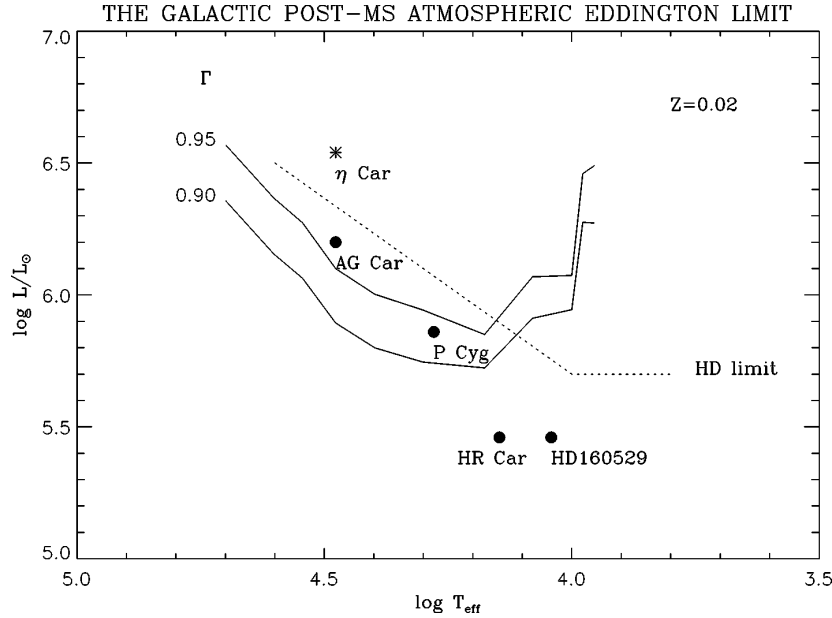

Figure 10.8: The empirical luminosity limit for hot stars found by Humphrey & Davidson, 1984 (dotted line) is well matched by the atmospheric Eddington limit (continuous lines). The parameter Γ is the Eddington factor given in eq. 10.40. The locations of a few well-known Luminous Blue Variables are indicated. (Figure reproduced from Massey 2003, ARA&A, 41, 15)
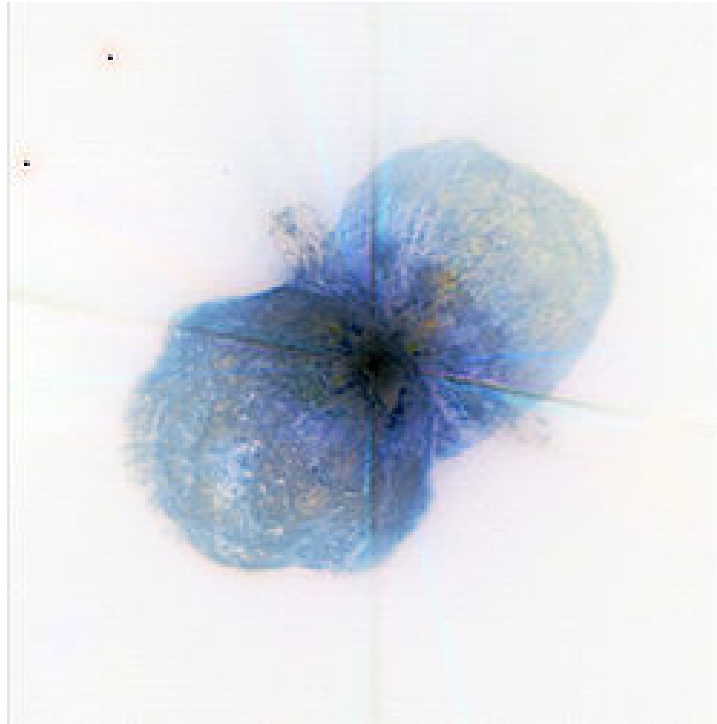
Figure 10.9: The star η Carinae is thought to be the closest example of a Luminous Blue Variable. It has recently been realised that it actually consists of at least two stars. η Carinae has undergone several periods of relative brightening and dimming in historical times; the last major outburst occurred in the 1840s, when the star reached visible magnitude $V = -0.8$, second only to Sirius (α CMa) which is $\sim$ 1000 times nearer to the Earth! The 1840s outburst, during which the star shed more than $1 M_\odot$, is thought to have created the Homunculus Nebula, seen in this spectacular image. Note the bipolarity of the outflow and the jets bisecting the lobes emanating from the central star. η Car still undergoes unexpected outbursts; its high mass and volatility make it a candidate to explode as a supernova sometime in the next few million years.

disrupted (as would be the case if they exceeded their classical Eddington limit), because it is only in the outer layers of the star that line opacity is effective in transferring momentum from the radiation field to matter.

The frequent (on an astronomical timescale) eruptions undergone by LBVs are recorded in the nebulae that surround them. The closest, and best studied, example is the star η Carinae in the Great Carina nebula, one of the regions of most intense star formation in the Milky Way, containing some of the most massive stars known (see Figure 10.9).

This concludes the part of the course which deals with stellar structure. In the next lectures we shall look in more detail at how stars form and at how they evolve during their lifetimes.